Electronic supplementary materials

For: https://doi.org/10.1631/jzus.A2200378

Theoretical and experimental investigation on the efficiency of a novel roller piston pump

Chenchen ZHANG, Yiren ZANG, Heyuan WANG, Bin MENG, Sheng LI, Jian RUAN✉

College of Mechanical Engineering, Zhejiang University of Technology, Hangzhou 310023, China

S1. Schematic diagram of the force of piston A under different load pressures when rotates from 45° to 90° and 90° to 135°

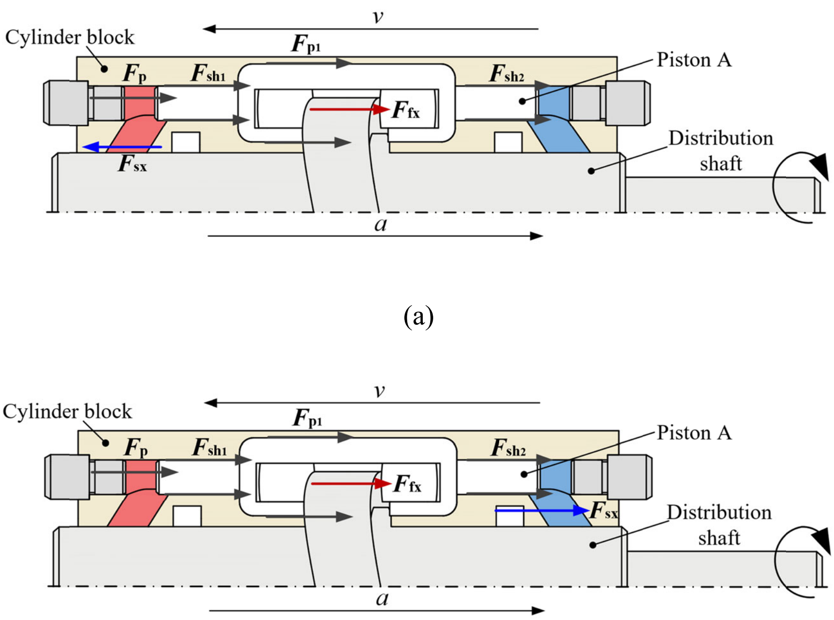

(a)

(b)

Fig. S1. Schematic diagram of the force of piston A under different load pressures when rotates from 45° to 90°

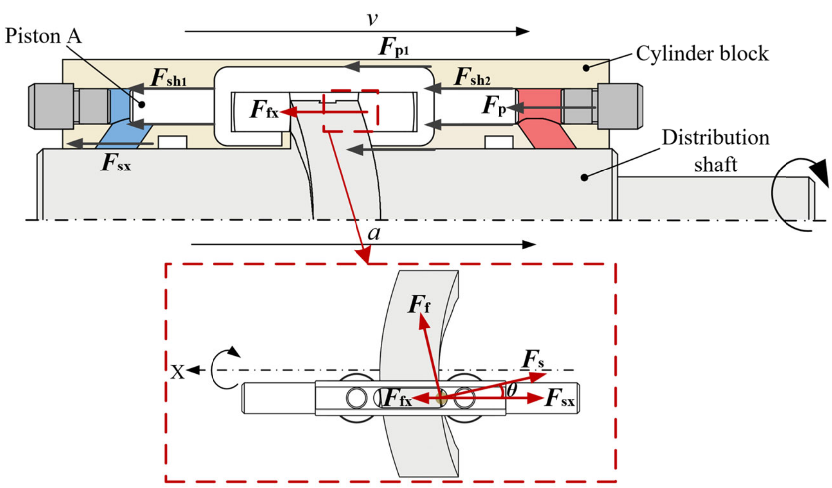

Fig. S2. Schematic diagram of the force of piston A when rotates from 90° to 135°

S2. Parameters for MATLAB and AMESim simulation

Table S1 Parameters for MATLAB and AMESim simulation.

Parameters	Value
Flow Coefficient C_d	0.62
Oil dynamic viscosity μ (Pa·s)	0.011
Oil modulus of elasticity β_e (MPa)	1000
Piston stroke h (m)	4×10^{-3}
Rolling friction coefficient μ_f	1×10^{-3}
Mass of piston A m (kg)	2.3×10^{-2}
Clearance width δ (m)	5×10^{-6}
Cylinder block outside diameter R (m)	2.1×10^{-2}
Diameter of piston rod D (m)	6.25×10^{-3}
Oil density ρ (kg/m^3)	840
Diameter of distribution shaft D_1 (m)	2.5×10^{-2}
Cross-sectional area of piston rod A (m^2)	3.06×10^{-5}
Displacement of the pump V_D (L/r)	3.925×10^{-3}
Contact length between distribution shaft and cylinder block L_3	5.8×10^{-3}

(m)	
Contact length between distribution shaft and cylinder block L_4 (m)	3.97×10^{-3}
Contact length between distribution shaft and cylinder block L_5 (m)	5.5×10^{-3}
Distance between high-pressure cavity and low-pressure annular flow channel L_6 (m)	3.97×10^{-3}
Total length of contact between the piston rod and the cylinder block $L(L_1+L_2)$ (m)	2.4×10^{-2}
Cross-sectional area of the piston on the left side of the rail S_1 (m^2)	5.63×10^{-5}
Cross-sectional area of the piston on the right side of the rail S_2 (m^2)	7.15×10^{-5}
Clearance between the side of the piston and the distribution shaft δ_1 (m)	5×10^{-4}
Maximum volume of working cavity V_{max} (m^3)	2.28×10^{-7}
Width of oil suction and discharge window on distribution shaft L_g (m)	7×10^{-3}
Minimum contact length between the piston rod and the left cylinder block L_{min} (m)	9.5×10^{-3}

S3. Detailed analysis of resistance torque simulation results for mechanical efficiency

First, the load pressure is 8 MPa and kept as constant. When the rotational speed of the pump increased from 1000 r/min to 10000 r/min, the input torque T of the pump drive assembly. Among them, the change of the sum of the input torque of the group I piston is shown in Fig. S3(a). Taking the rotation at 45° as the dividing line, when the guide rail rotates from 0° to 45°, the generated inertial force hinders the rotation, so more torque is required to maintain the rotation, and the input torque increases linearly during this process. When the rotation reaches at 45°, the acceleration of the piston of group I is reversed, resulting in a sudden change in the input torque. It is known that as rotational speed increases, so does acceleration, so the faster the rotational speed, the greater the sudden change of the input torque. When the guide rail rotates from 45° to 90°, the required torque decreases due to inertial forces assisting the rotation. Fig. S3(b) shows the variation of the sum of the input torques of the group II pistons with the rotational speed, and its change rule is basically the same as that of the group I pistons.

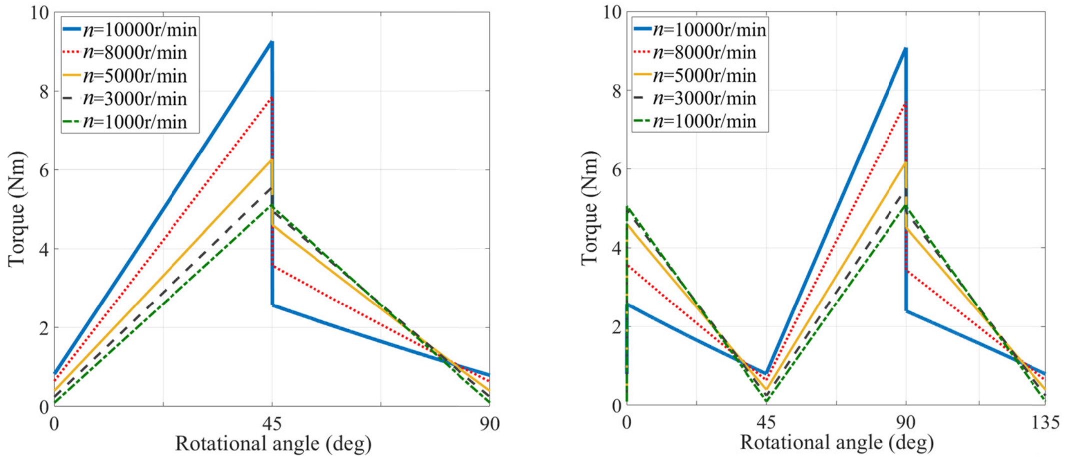

(a) Sum of input torque of group I pistons (b) Sum of input torque of group II pistons

Fig. S3. Variation of pump input torque with rotational speed when the load pressure is 8MPa

In order to study the effect of load pressure on the pump input torque, it is assumed that when the rotational speed is 8000 r/min, the change of input torque under different load pressures is shown in Fig. S4. When the rotational speed is constant, the input torque of the group I pistons and the group II pistons increase with the load pressure, which is primarily caused by the increasing of the force of the high-pressure cavity on the pistons. Due to the installation phase difference of the pistons, when the group II pistons rotate to 90°, the acceleration is reversed, resulting in a sudden change of torque, as shown in Fig. S4(b).

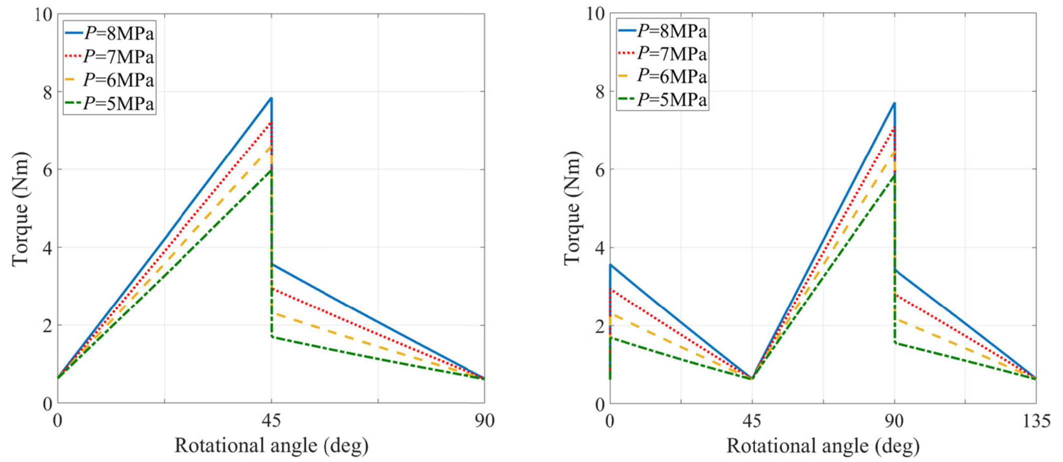

(a) Sum of input torque of group I pistons (b) Sum of input torque of group II pistons

Fig. S4. Variation of pump input torque with load pressure when the rotational speed is 8000 r/min

S4. Detailed analysis of leakage simulation results for volumetric efficiency

When the piston A rotates from 0° to 90°, the left cavity discharges oil, and when 90° to 180°, the left cavity suctions oil. Fig. S5 and S6 show the change curves of Q_{Lo1} under different rotational speeds and load pressures, respectively. Q_{Lo1} consists of leakage Q_{Lo11} due to differential pressure flow and Q_{Lo12} leakage due to shear flow. When the working cavity finishes absorbing oil and is about to start discharging oil, the backflow helps to rapidly increase the pressure in the working cavity. Subsequently, with the increase of the contact length of the piston rod and the cylinder block and the axial movement speed of the piston A, Q_{Lo11} decreases and Q_{Lo12} increases, and Q_{Lo1} decreases after superposition. When the rotation exceeds 45°, due to the decrease in the axial movement speed of the piston A, the Q_{Lo12} decreases. Q_{Lo1} decreases slowly, and even begins to increase. During the oil discharge phase, the directions of Q_{Lo11} and Q_{Lo12} are opposite, so that Q_{Lo1} decreases as the speed increases. The oil suction stage Q_{Lo1} only includes Q_{Lo12}, and at this time Q_{Lo1} increases with the increase of the rotational speed, as shown in **Fig. S5(c)**. When the speed remains the same, in the oil discharge phase, Q_{Lo1} increases with the increase of load pressure. During the oil suction stage, Q_{Lo1} does not change with the load pressure.

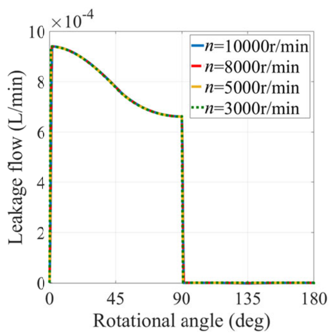

(a) Q_{Lo11}

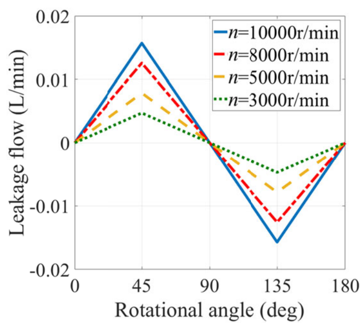

(b) Q_{Lo12}

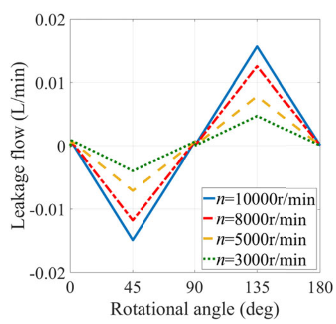

(c) Q_{Lo1}

Fig. S5. Q_{Lo1} under different rotational speeds at 8MPa

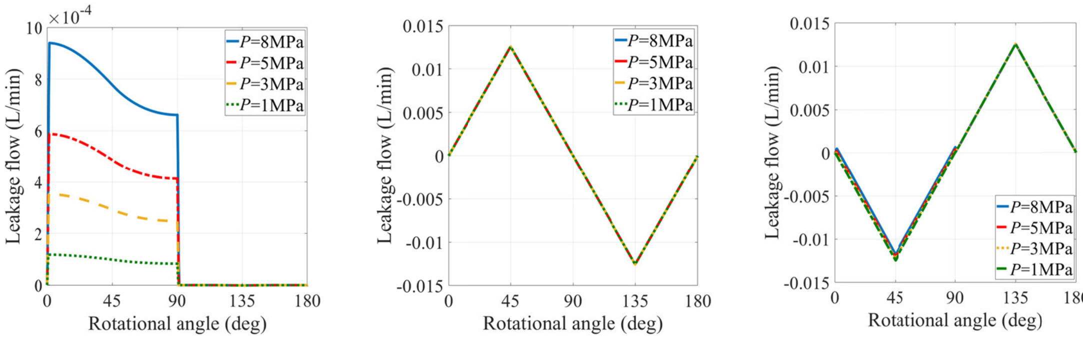

(a) Q_{Lo11} (b) Q_{Lo12} (c) Q_{Lo1}

Fig. S6. Q_{Lo1} under different load pressures at 8000 r/min

Q_{Lo2} is the external leakage between the outer wall of the cylinder block and the outer wall of the distribution shaft, and Q_{Li1} is the axial internal leakage caused by the clearance between the outer wall of the distribution shaft and the inner wall of the cylinder block. Since the contact length is constant and there is no relative velocity, leakage does not vary with rotational speed. Both Q_{Lo2} and Q_{Li1} are leakages caused by differential pressure flow, so in the oil discharge stage, and when the speed is constant at 8000 r/min and the load pressure increases, Q_{Lo2} and Q_{Li1} rise, as shown in Fig. S7.

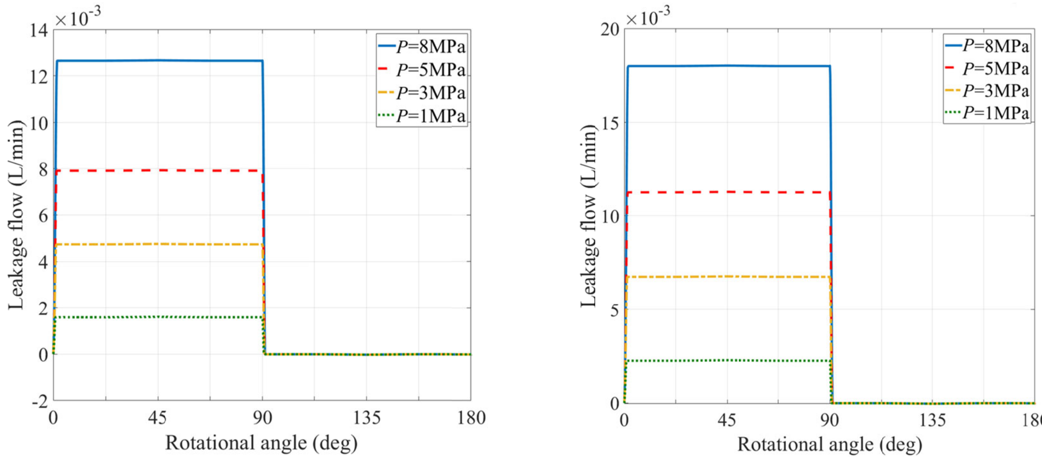

(a) Q_{Lo2} (b) Q_{Li1}

Fig. S7. Q_{Lo2} and Q_{Li1} under different load pressures at 8000 r/min

Fig. S8 illustrates the effect of rotational speed and load pressure on the internal circumferential leakage Q_{Li2}. Leak curve shows a satisfying consistence between the theoretical findings and simulation results. When the roller piston pump is rotates at 0°, 45°, 90° and 135°, instantaneous leakage occurs. At this time, the seal between the cylinder block and the distribution shaft changes from face-seal to linear sealing, and this moment the leakage is caused by small hole leak. The instantaneous leakage flow rate does not change significantly with the increase of rotational speed, but the peak value of backflow rises slightly with the increase of rotational speed, as shown in Fig. S8(a). In addition, as the load pressure goes up, the instantaneous leakage value rises due to the increasing in the pressure difference between the tank and high-pressure cavity, as shown in Fig. S8(b).

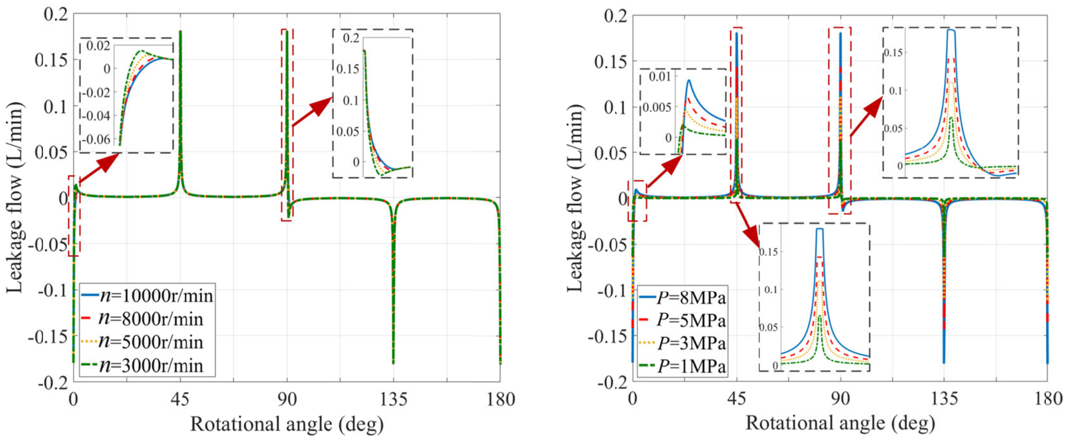

(a) Different rotational speeds when load pressure is 8 MPa

(b) Different load pressures when rotational speed is 8000 r/min

Fig. S8. Q_{Li2} at different rotational speeds and load pressures

S5. Parameters of main test instruments

Table S2 Parameters of main test instruments

Name	Parameter
VSE Flow meter	range 0.05-80L/min，precision ±0.3%
SL06 torque-speed sensor	range 0-20Nm，precision ±0.1%，rotational speed 0-18000r/min
MIK-P300 pressure sensor	Range 0-10MPa，precision ±0.3%

S6. Parameter appendix table

Table S3 Nomenclature

n	Rotational speed	D	Diameter of the piston rod
t	Rotational time	D_1	Diameter of distribution shaft
$t_{90°}$	Time required for the moving components to rotate from 0° to 90°	R	Radius of the guide rail
h	Stroke of piston	L	Total length of contact between the piston rod and the cylinder block
v	Speed of the axial movement of the piston A	L_1	Contact length of the left piston rod and the cylinder block
a	Acceleration of the axial movement of the piston A	L_2	Contact length of the right piston rod and the cylinder block
F_p	Thrust of the high-pressure cavity to the piston A	L_3	Contact length between distribution shaft and cylinder block
F_{sh}	Oil shearing force between the piston A and the cylinder block	L_4	Contact length between distribution shaft and cylinder block
F_{p1}	Resistance when the piston A moves axially	L_5	Contact length between distribution shaft and cylinder block
F_s	Support force between the cylindrical roller and the guide rail	L_6	Distance between high-pressure cavity and low-pressure annular flow channel
F_f	Frictional force	L_g	Width of oil suction and discharge window on distribution shaft
F_{sx}	Support force of the guide rail on the axial direction of the piston A	L_r	Contact length between the distribution shaft and the cylinder block
F_{fx}	Frictional force of the guide rail on the axial direction of the piston A	L_{min}	Minimum contact length between the piston rod and the left cylinder block
m	Mass of piston A	S_1	Cross-sectional area of the piston on the left side of the rail
p_L	Instantaneous pressure in the left cavity of piston A	S_2	Cross-sectional area of the piston on the right side of the rail
P	Load pressure	δ	Clearance width
A	Cross-sectional area of the left piston rod	δ_1	Clearance between the side of the piston and the distribution shaft
μ	Oil dynamic viscosity	β_e	Oil modulus of elasticity
μ_f	Rolling friction coefficient	C_d	Flow Coefficient
θ	Pressure angle	Q_o	Output flow of the left cavity
T_{i1}	Torque of piston A at rotation from 0°	Q_i	Input flow of the left cavity

	to 45°		
T_s	Shear resistance torque	Q_{oT}	Total discharge flow of roller piston pump
T_c	Churning loss torque	Q_{LT}	Leakage of roller piston pump
T_{i2}	Torque of piston A at rotation from 45° to 90°	Q_L	Leakage of piston A
T	Torque of roller piston pump	Q_{LL}	Leakage of left cavity
η_m	Mechanical efficiency of roller piston pump	Q_{Lo}	External leakage
η_v	Volumetric efficiency of roller piston pump	Q_{Li}	Internal leakage
V_D	Displacement of roller piston pump	V_L	Instantaneous volume of the left cavity
V_{max}	Maximum volume of working cavity	p_T	Tank pressure
ρ	Oil density	Δp_{rs}	Difference between the high-pressure cavity pressure and the ambient pressure
A_{in}	Communication areas between distribution cylinder and suction ports	A_{out}	Communication areas between distribution cylinder and discharge ports
Q_{Lo1}	Outward leakage of the high-pressure cavity oil through the clearance between the outer wall of the piston rod and the inner wall of the cylinder block	Q_{Lo2}	Outward leakage from the clearance between the outer wall of the cylinder block and the outer wall of the distribution shaft
Q_{Li1}	Internal leakage produced by the clearance between the outer wall of distribution shaft and cylinder block	Q_{Li2}	Circumferential internal leakage caused by the clearance between the outer wall of distribution shaft and cylinder block
		Δp_p	Difference between the high-pressure cavity of the piston and the low-pressure annular flow channel